Noble gas temperature control of metal clusters: A molecular dynamics study

Jan Westergren and Henrik Grönbeck
Department of Physics, Göteborg University and Chalmers University of Technology, S-412 96 Göteborg, Sweden

Seong-Gon Kim[a] and David Tománek
Department of Physics and Astronomy, Michigan State University, East Lansing, Michigan 48824-1116

(Received 23 April 1997; accepted 19 May 1997)

We use classical molecular dynamics simulations to investigate temperature control of unsupported clusters using a noble gas atmosphere. The simulations are performed using a many-body interaction scheme for the intra-cluster potential, while a pairwise Lennard-Jones potential is used to model the interaction between the noble gas and the clusters. In order to isolate different parameters determining the energy exchange efficiency, we have studied the energy transfer with respect to (i) impact parameter, (ii) cluster temperature, (iii) noble gas temperature, (iv) gas–metal interaction strength, (v) metal potential, and (vi) noble gas mass. With these results, we are able to estimate the number of collisions needed to equilibrate a cluster at a given gas temperature. Our estimates are confirmed by simulations of cluster cooling in a noble gas atmosphere. © *1997 American Institute of Physics.* [S0021-9606(97)50332-1]

I. INTRODUCTION

Temperature control of unsupported atomic clusters is of crucial importance, since several properties have been reported to strongly depend on the internal cluster energy. Observables showing a marked temperature dependence include ionization potentials,[1] magnetic moments,[2] and reactivity.[3]

Clusters are commonly produced with the laser-vaporization technique.[4] In this method a metal target is vaporized, and clusters form by condensing from the gas phase in the presence of a thermalizing buffer gas, usually helium. A cluster beam forms during a subsequent supersonic expansion through a nozzle, which cools the aggregating clusters and the carrier gas. The heat of condensation is carried away in collisions with the ''cold'' buffer gas. Consequently, the temperature of the clusters is determined by the number of collisions with the buffer gas in the source (controlled by pressure and residence time), and the supersonic expansion (determined by pressure difference and nozzle configuration). Important to notice, however, is that the two mechanisms used for controlling the cluster temperature may couple differently to vibrational, translational, and rotational modes of the clusters. While we can expect equal partitioning of energy over all the different degrees of freedom in the source, supersonic expansion is known to cool only translations and rotations efficiently,[5] while the clusters could retain a vibrational temperature close to the source temperature.

Experimentally it has not yet been possible to measure the internal cluster temperatures, although ''liquid'' clusters could be distinguished from ''rigid'' by adsorbing weakly bound adsorbates.[6,7] Estimates of cluster temperature have mainly followed arguments based on the number of collisions experienced by the clusters with the buffer gas in the source. However, a detailed knowledge about energy exchange efficiency in the case of metal clusters, and, in particular, the effect of the different parameters on the efficiency, is missing.

In the present paper we address these problems by molecular dynamics (MD) simulations, calculating classical trajectories of collisions between noble gas atoms and metal clusters. In the simulations we investigate the efficiency of the energy transfer as a function of several key parameters, including (i) impact parameter, (ii) cluster temperature, (iii) noble gas temperature, (iv) gas–metal interaction strength, (v) metal potential, and (vi) the mass of noble gas atoms. As a cluster model system we use an icosahedral 13-atom cluster. In our simulations the intra-cluster potential is based on the second moment approximation of a tight-binding total-energy functional, the many-body alloy (MBA) potential.[8,9] The noble gas–metal potential is, on the other hand, described by a pairwise Lennard-Jones potential. By evaluating the mean energy exchange for the different situations we are able to put forth a simple relation for the energy exchange between the buffer gas and an atomic cluster. Our results are also discussed in the context of analytical model expressions that have appeared in the literature.[10–12] We apply the results from the simulations to estimate the number of collisions that are needed for a noble gas to thermalize a cluster to a low source temperature. Moreover, using a low cooling rate, the ''fluid'' to ''rigid'' transition in a Pd_{13} cluster is studied, taking a cluster with high atomic diffusion below the ''freezing'' temperature. Our results are in agreement with reported simulations[13] using a Nosé–Hoover thermostat both for the transition temperature and the width of the co-existence region.

Energy transfer in molecular collisions is also of fundamental importance within the field of thermal unimolecular reactions, and MD simulations have been used to address the

[a]Present address: Complex Systems Theory Branch, Naval Research Laboratory, Washington, D.C. 20375-5000.

energy transfer in collisions between noble gas atoms and mostly small molecules.[14,15] For metal clusters, however, the dynamics of collisions and energy transfer have only recently become the subject of investigations.[16,17] Schulte *et al.*[16] studied the energy equilibration in a small Mo_5 cluster, where both the intercluster and the cluster–gas potential were modeled by pairwise interactions. In this study the authors investigated the effect of mass of the collider and the strength of the cluster–noble gas interaction. Sainte Claire *et al.*[17] studied the energy transfer in the high collision energy limit with the aim to interpret collision induced dissociation experiments of small aluminum clusters. In the present work we extend the previous studies by studying the dynamics in the thermal regime, where gas–cluster collisions are used for controlling the cluster temperature, using potentials which incorporate many-body effects.

II. COMPUTATIONAL DETAILS

A. Interaction potentials

Although the applicability of *ab initio* theories has increased during the last decade, collision studies on an *ab initio* level have appeared only for small systems,[18] and the issue addressed in this work is still computationally too demanding for an *ab initio* treatment. Instead, we use a reliable model potential. For this purpose we have adopted the MBA potential.[8,9] This potential consists of a many-body binding term, based on the second-moment approximation for the electronic density of states, and pairwise repulsive Born–Mayer interactions. The potential energy for metal atom i, situated at distances r_{ij} from neighboring atoms, is given by

$$V(i)=-\left\{\sum_{i\neq j}\xi_0^2 e^{-2q(r_{ij}/r_0-1)}\right\}^{1/2}+\sum_{i\neq j}\epsilon_0 e^{-p(r_{ij}/r_0-1)}. \tag{1}$$

The first part represents the many-body binding term, and the second the pairwise repulsion. The parameters, ξ_0, ϵ_0, p, q, and r_0 have been determined by fitting to *ab initio* local density functional results for bulk Pd.[9] In this way the MBA potential reproduces the bulk values for lattice constant and cohesive energy at zero temperature. The validity of using this potential at finite temperatures is demonstrated by reproducing the experimental melting temperature of bulk Pd within 150 K.[19] For finite systems, such as Pd_{13}, this potential compares favorably with SCF-CI calculations[20] of the optimized geometry. The MBA value of 2.50 Å for the mean radius of the Pd_{13} icosahedron is close to the SCF-CI value of 2.60 Å, and the energy difference between the icosahedral and the octahedral isomers is 0.12 eV in both techniques.

In order to study the effect of the intra-cluster potential on the collision efficiency, we have modified the parameters of Eq. (1) to obtain a softer potential with a shallower potential well. This new set of parameters resembles those describing bulk sodium.[21] However, since the performance of this type of potential for small free electron clusters is questionable, we refer to this choice of parameters as the ''soft potential'' case. The difference between the potentials could be measured in the different harmonic vibration frequency for the metal dimer. For Pd_2 and the soft potential case using Pd mass, the vibrational frequencies are 218 cm^{-1} and 80 cm^{-1}, respectively.

For the interaction between the gas and the cluster atoms we used the pairwise Lennard-Jones potential,

$$V(i)=\sum_{j\neq i}4\epsilon_{\mathrm{LJ}}\left(\left(\frac{\sigma_{\mathrm{LJ}}}{r_{ij}}\right)^{12}-\left(\frac{\sigma_{\mathrm{LJ}}}{r_{ij}}\right)^{6}\right). \tag{2}$$

We here use helium parameters, i.e., $\epsilon_{\mathrm{LJ}}=0.88075$ meV and $\sigma_{\mathrm{LJ}}=2.6$ Å.

B. Simulation set-up

The energy transfer in the gas–cluster collisions is evaluated by performing classical trajectory simulations. The trajectories are obtained by integrating Newton's equations of motion using a fourth order Runge–Kutta algorithm.[22] Since some of the collisions are fast, we have used a small time step of 0.5 fs to ensure conservation of the total energy E. With this choice of time step, $\Delta E/E$ is about 10^{-10}.

The collisions are performed on an ensemble of cluster configurations obtained from microcanonical simulations of bare clusters corresponding to two different cluster temperatures, namely 100 and 500 K. Here we use the term ''corresponding'' since the cluster at a specific temperature has a distribution in total energy, although rather narrow. The total energy set in the microcanonical simulation is the mean total energy at T_c (see below).

The initial cluster configurations picked from the microcanonical ensemble have the entire kinetic energy distributed in the vibrational modes, i.e. the cluster has initially no rotation nor center of mass (CM) translation. By this choice we may easily investigate the amount of energy transferred into rotational or translational modes. In Appendix A we show how it is possible to correct for an initial translation after the simulations. The total cluster temperature is related to the kinetic energy according to

$$\frac{3n}{2}k_bT_c=\left\langle\sum_{i=1}^{n}\frac{m_iv_i^2}{2}\right\rangle. \tag{3}$$

m_i is the mass of the metal atoms (106.4 amu for Pd) and n is the number of metal atoms ($n=13$ in our case). k_b is Boltzmann's constant.

When setting up the collisions, the starting position of the gas atoms is randomly chosen under the constraint that the distance between the gas and the nearest metal atom is equal to a cut-off distance for the interaction, i.e., the distance where the interaction between the gas atom and a metal atom can be ignored. The velocity towards the cluster is randomly chosen, but generated so that the impact parameter b follows a specific distribution with max $b=b_{\max}$, and the speed follows the velocity weighted Maxwell–Boltzmann distribution (see below).

After the collision event, when the gas atom has left the interaction zone, the system is evolved to collect statistics of the cluster. During this time the energies in the different

modes of motion in the cluster are sampled. The energies transferred into the different modes are calculated as

$$\epsilon_{\mathrm{vib}}=\langle e_{\mathrm{vib}}\rangle-e_{\mathrm{vib}},$$

$$\epsilon_{\mathrm{cm}}=\langle e_{\mathrm{cm}}\rangle,$$

$$\epsilon_{\mathrm{rot}}=\langle e_{\mathrm{rot}}\rangle,$$

$$\epsilon=\epsilon_{\mathrm{vib}}+\epsilon_{\mathrm{cm}}+\epsilon_{\mathrm{rot}}.$$

$\langle e_{\mathrm{vib}}\rangle$ is the time average during the sampling and e_{vib} the initial vibrational energy. e_{vib} consists of a potential and a kinetic part. The total energy transfer ϵ is, of course, equal to the change in the kinetic energy of the gas atom $(e_g-e_{g,f})$, where e_g and $e_{g,f}$ are the initial and final kinetic energies.

For each set of input parameters we have performed 30 000 collisions, which gives us good statistics. By taking averages over $\epsilon, \epsilon_{\mathrm{vib}}, \epsilon_{\mathrm{rot}}$, and ϵ_{cm} we are able to estimate the energy transfer per collision in a realistic gas.

In our simulations only one atom is colliding with the cluster at a time. It is important to know above what pressure the number of collisions with more than one gas atom colliding at the same time is unacceptably high. In Appendix B we conclude that for a gas of temperature $T_g=300$ K and below the pressure $p_g=150$ mbar, more than 98% are single collisions, which we consider acceptable. The experimental pressure in a laser vaporization source is usually about 100 mbar.

C. Statistics

As described above, a collision is defined as a gas atom passing through a sphere with radius b_{max}, having its center in the center-of-mass point of the cluster. b_{max} is set so that the energy transfer between the gas atom and the metal atoms is negligible when the gas atom passes outside the sphere.

Here we focus on the total energy transfer from the gas atom to the cluster, ϵ. (The vibrational, CM, and rotational energy transfers follow the same reasoning.) The outcome of a collision event is three stochastic quantities: the initial speed of the gas atom, v, the impact parameter, b, and ϵ. v and b are independent of each other and of ϵ, having known distribution functions, while the distribution of ϵ depends on both v and b. The distribution of v depends on the considered temperature of the gas, T_g, according to the velocity weighted Maxwell–Boltzmann distribution for the colliding gas.

The mean energy transfer is given by

$$\overline{\epsilon}(T_g)=\int_0^{b_{\mathrm{max}}}db\int_0^{\infty}dv\int_{-\infty}^{\infty}d\epsilon \times f_b(b)f_v(v,T_g)f_\epsilon(\epsilon,b,v)\cdot\epsilon, \tag{4}$$

where the distribution functions are

$$f_b(b)=\frac{2}{b_{\mathrm{max}}^2}b,$$

$$f_v(v,T_g)=\frac{m^2}{2k_b^2T_g^2}v^3e^{-mv^2/2k_bT_g},$$

f_ϵ, unknown.

Here, m is the mass of the gas atom.

For large v, $f_v(v,T_g)$ is small, and therefore we change the upper integration limit from infinity to v_{99}. At least 99% of the gas atoms have a speed lower than v_{99}. The value of v_{99} is determined by the upper bound of the temperature interval which we are simulating, [100 K, 900 K].

Since large b contribute in a minor fashion to $\overline{\epsilon}$, it is desirable to generate fewer trajectories for large b than suggested by the f_b distribution. Also, it is inconvenient to specify T_g before the simulations, as f_v requires. Thus, instead of using f_b and f_v for the generation of the starting configurations, we introduce new distributions $\tilde{f}_b(b)$ and $\tilde{f}_v(v)$. $\tilde{f}_b(b)$ is given by

$$\tilde{f}_b(b)=\frac{1}{b_{\mathrm{max}}}, \tag{5}$$

and $\tilde{f}_v(v)$ is a stepwise linear function of e_g and independent of T_g, being a compromise between the functions $f(v;T_g)$ for $T_g \in$ [100 K, 900 K].

From the trajectory simulations the average of the energy transfers is now calculated according to

$$\overline{\epsilon}(T_g)=\int_0^{b_{\mathrm{max}}}db\int_0^{v_{99}}dv\int_{-\infty}^{\infty}d\epsilon\frac{f_b(b)f_v(v,T_g)}{\tilde{f}_b(b)\tilde{f}_v(v)} \times\tilde{f}_b(b)\tilde{f}_v(v)f_\epsilon(\epsilon,b,v)\cdot\epsilon \approx\frac{1}{N}\sum_{i=1}^{N}g(b_i,v_i,T_g)\cdot\epsilon_i, \tag{6}$$

where

$$g(b_i,v_i,T_g)=\frac{f_b(b_i)f_v(v_i,T_g)}{\tilde{f}_b(b_i)\tilde{f}_v(v_i)}, \tag{7}$$

and N is the number of collisions.

With this expression it is possible to estimate $\overline{\epsilon}$ for different T_g using the same set $\{b_i,v_i,\epsilon_i\}$, only recalculating the analytically known weight coefficients $\{g(b_i,v_i,T_g)\}$.

From Eq. (6) we can see that an increase of b_{max} will just add extra trajectories having $\epsilon=0$, reducing $\overline{\epsilon}$. Hence, $\overline{\epsilon}$ is dependent on the choice of b_{max}. However, $\overline{\epsilon}\cdot b_{\mathrm{max}}^2$ is a b_{max}-independent quantity which we use when presenting our results,

$$\overline{\epsilon}_{\mathrm{norm}}=\overline{\epsilon}\cdot\left(\frac{b_{\mathrm{max}}}{b_0}\right)^2, \tag{8}$$

where we have chosen $b_0=6.5$ Å.

D. Error estimation

The standard deviation estimation of ϵ sampled from N collisions is

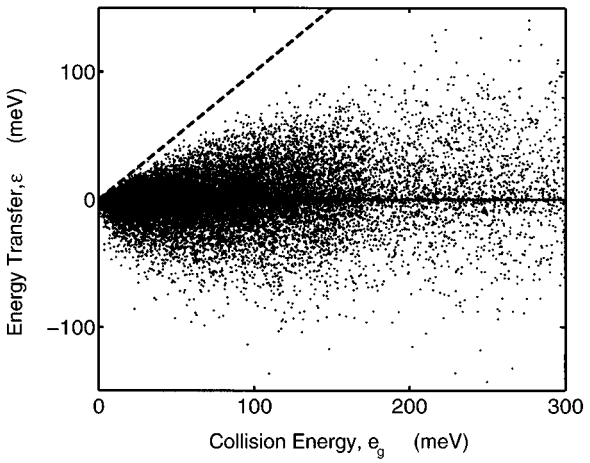

FIG. 1. Total energy transfer ϵ versus the initial kinetic energy of the helium atom, e_g. The collisions were performed on cluster configurations taken from a microcanonical simulation with the cluster at 500 K.

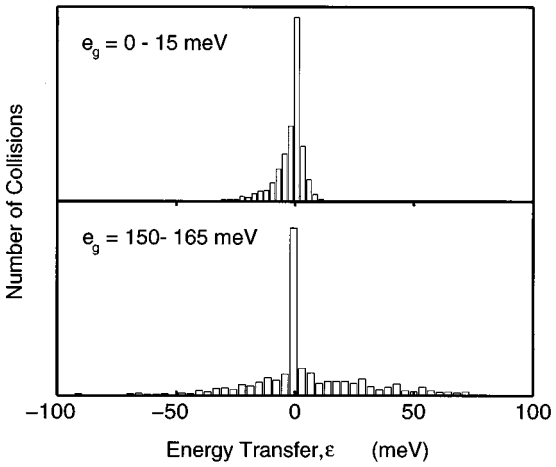

FIG. 2. Histograms for the data points for the collisions in Fig. 1, taken at two energy intervals.

$$s_\epsilon^2(T_g)=\frac{1}{N}\sum_{i=1}^{N}(g_i(T_g)\cdot\epsilon_i^2)-\overline{\epsilon^2}. \tag{9}$$

As an error estimation for $\overline{\epsilon}_{\text{norm}}$ in the graphs we use

$$S_{\text{norm}}=\frac{s_\epsilon(T_g)}{\sqrt{N}}\left(\frac{b_{\max}}{b_0}\right)^2. \tag{10}$$

III. RESULTS AND DISCUSSION

A. Influence of interaction strengths, mass, and temperature

The outcome of a single collision is determined by the cluster temperature, collision energy, as well as the impact parameter. Of experimental significance is, of course, the *average* properties, i.e., the mean energy transfer for certain temperatures of the cluster and the noble gas. However, to understand the average quantities it is illuminating to study the energy exchange of single trajectories, which we do in Figs. 1 and 2.

The first system we investigate is Pd_{13} in collisions with helium. In Fig. 1 the total energy transfer, ϵ, as a function of initial kinetic energy of the helium atoms (collision energy) is displayed. As a reference we indicate the maximal energy transfer as a straight line, corresponding to a collision where the gas atom transfers all its kinetic energy to the cluster. A large fraction of the collision events result in an energy transfer close to zero. This is to the largest extent due to trajectories with large impact parameters, giving a weak interaction with the cluster. It is important to notice the asymmetry in the energy transfer cloud: Negative energy transfer (heating of the gas atom) does not appear to have a limiting value as the positive energy transfer has. It is not surprising that the maximum energy transfer overestimates the simulated maximum exchange for all collision energies, except in the limit of small e_g.

The asymmetry in the energy exchange is more clearly seen if the data is exposed in histograms, Fig. 2. Here, data points for collisions with collision energies within two energy intervals, [0,15 meV] and [150,165 meV] are shown. Both distributions are peaked close to a zero energy transfer. For the low collision energy (upper panel) the distribution is expanding towards negative energy transfers. This has changed in the high energy case (lower panel). Not only the expectation value has increased but the distribution is distinctly broader, with a modified shape. Even though the collision energy is higher in the lower panel, several trajectories result in a negative energy exchange with the cluster.

Knowing that trajectories with large impact parameters give zero energy exchange, it is desirable to know the influence of the impact parameter on the energy transfer, both the shape of this function, and its radial extension. The energy transfer as a function of impact parameter, b, is shown in Fig. 3 for the two cases of a hard and a soft intra-cluster potential. The noble gas atoms were in both cases helium.

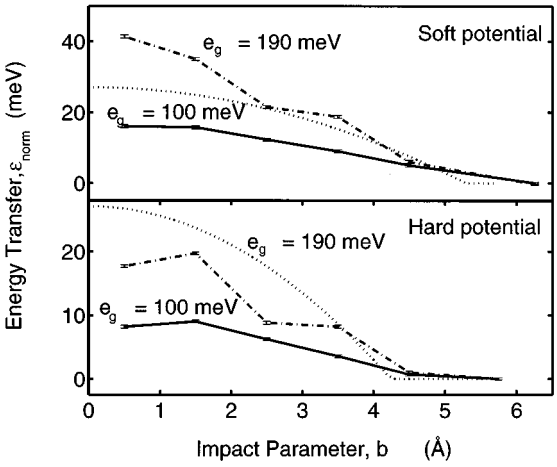

FIG. 3. The energy transfer as a function of impact parameter. The lower panel shows the results for the cluster with a hard (Pd) intra-cluster potential, while the upper panel is with the soft (Na) potential. In both cases a Pd mass was used. The temperature of the cluster is in both cases 100 K.

Note that the metal–gas potential was kept the same in the two sets of data presented.

The collision energies e_g were selected so that $2e_g/3k_b \in [T-50, T+50]$, where $T=800$ and 1500 K, respectively. Comparing the high and low collision energy cases, it is seen how a high e_g is probing the structure of the cluster, while the low collision energy only results in a smooth energy transfer profile. This holds for both the soft and the hard intra-cluster potential. Effects of the metal potential are instead observed in the absolute energy transfer to the cluster. In the soft potential case, the energy exchange is about twice that of the hard potential. This is in agreement with previous simulations performed at high collision energies.[17] These authors related this effect to the analytical model by Mahan[10] for translational to vibrational energy exchange of a diatomic oscillator. The model gives a relation of how the energy transfer is reduced with increasing vibration frequency (keeping the other parameters constant).

In cluster scattering experiments, clusters are commonly modeled as hard spheres.[23] The radius of the cluster is in such approaches estimated from the Wigner–Seitz radius of the metal and the number of atoms in the cluster. Our calculations offer a possibility to compare the hard sphere model with the more realistic effective radius, given by the interaction potentials used in the simulations. In Fig. 3 the result from the simulations are compared with the energy expression from a hard sphere model[24] with $e_g=190$ meV, dotted lines. The absolute value of the energy transfer is in the hard sphere model a function of the ''effective'' mass of the cluster experienced by the gas atom.[12] Here we have used the mass of a single palladium atom. The hard sphere energy exchange profile resembles the smooth low collision energy profile. The largest impact parameter contributing to the mean energy transfer, is 6.5 and 5.5 Å for the soft and the hard potential, respectively. This could be compared with the hard sphere radii, being 5.3 and 4.2 Å, respectively.

The amount of energy transferred in a collision may couple differently with the different degrees of freedom: vibrations, rigid rotations, and center of mass translations. In Fig. 4, the energy transfer $\overline{\epsilon}_{\text{norm}}$ is resolved into these different degrees of freedom in the case of Pd_{13} colliding with helium atoms. The energy transfer is given as a function of gas temperature, and the cluster temperature is 500 K. A zero energy exchange is found in the total energy for a gas temperature of 500 K. In the vibrations, this cross over occurs at 600 K, which is a result of that all kinetic energy of the cluster, initially is in the vibrational degrees of freedom of the cluster. This results also in an overall positive energy transfer to rotations and translations. The slope of the energy transfer into translations are larger than that for the rotations. The slope for the rotations and the vibrations are, on the other hand close, taking into account the large difference in degrees of freedom, 3 versus 33.

Helium is commonly used as buffer gas in cluster sources.[6] Helium is light, and a larger energy exchange per collision would actually be assumed if the gas atoms were heavier, choosing argon or neon. To investigate this, we performed a set of simulations where the mass of the gas atoms

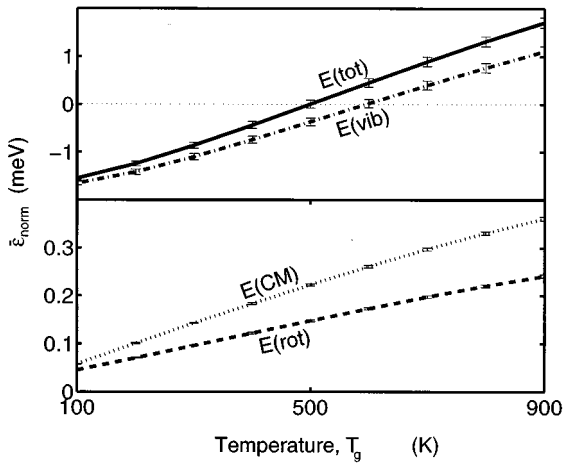

FIG. 4. Helium atom collisions with Pd_{13} at 500 K. The upper panel shows total and vibrational energy. The lower panel corresponds to rotational and translational energy transfer.

were varied, keeping the Lennard-Jones interaction parameters fixed. In Fig. 5, the results for collisions with Pd_{13} are shown. In addition to helium (4.003 amu) the gas mass equals neon (20.18 amu) and argon (39.95 amu). The upper panel shows the cluster at an initial temperature of 100 K, and the lower panel the cluster at 500 K. The cross over from negative to positive energy transfer is shifted for the three different cases. This is, however, an effect of displaying the *total* energy transfer. For the vibrational degrees of freedom, the cross over occurs at the temperature of vibrations, namely 600 K in all cases. We find that the larger the mass, the larger amount of energy is transferred to the clusters. The curves show two regions: At low temperatures the energy transfer is non-linear with respect to the gas temperatures, and at high gas temperatures the transfer appears to reach a linear behavior. It is obvious that the non-linear region is reflecting the differences in the absolute velocity distributions for the different gases at a given temperature. For the

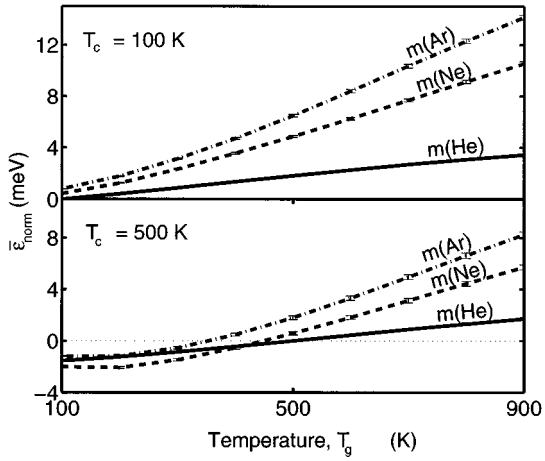

FIG. 5. The total energy transfer, as a function of gas temperature, for three different masses of the noble gas atoms. The cluster is initially at 100 and 500 K.

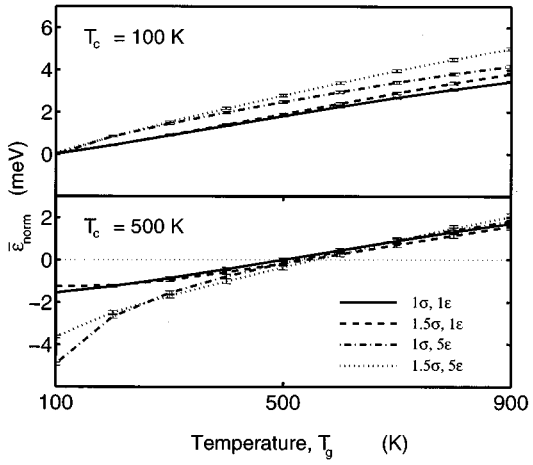

FIG. 6. The influence of the interaction strength in the Lennard-Jones intermolecular potential. σ and ϵ correspond to the values for helium given in the text.

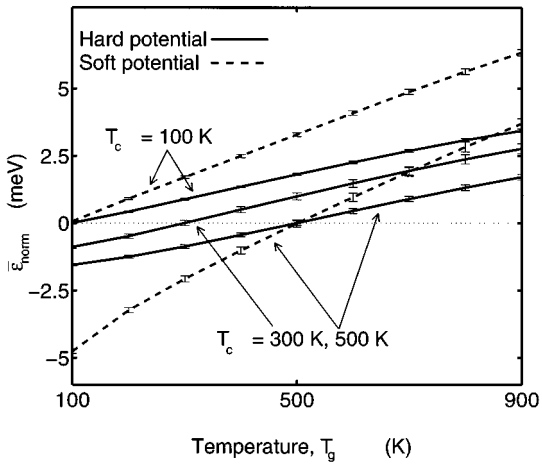

FIG. 7. The influence of the intra-cluster potential. The gas mass was 4.003 amu and the gas–cluster potential was the Lennard-Jones of He.

heavier atoms, the velocities at low temperatures are of the same magnitude as the metal atoms in their vibrations. This gives a resonance in the collision events, reducing the cluster cooling.

We notice that the hard sphere estimation for the difference in energy exchange is out of order if the total mass of the cluster is taken into account.[24] For example, a factor ten in difference between helium and argon is predicted by the hard sphere model, while the simulations indicate a factor four in the linear region. If instead we use the cluster mass as an adjustable parameter, fitting the difference in energy exchange having different noble gas masses, we find a perfect agreement using the mass of a single Pd atom scaled with 1.75. In fact, this is in close agreement with the work by Grimmelmann *et al.*[12] These authors were able to fit experimental argon scattering data on tungsten surfaces using a hard cube model where the effective surface mass was 1.5 times that of a tungsten atom.

To examine the influence of the interaction between the gas atom and the cluster atoms we performed a series of simulations with the gas mass kept to helium mass and the hard cluster potential fixed, while the Lennard-Jones potential between the gas and the cluster atom was varied, Fig. 6. In the heating regions the effect of different potentials was found to be minor. However, having a large ϵ_{LJ} and a small σ_{LJ}, i.e., a potential well which is deep and narrow is advantageous for an efficient cooling of the cluster. For the energy exchange into rotations we find that the potential with large σ_{LJ} reduces the excitations of the rotations compared with $\sigma_{\mathrm{LJ,\,He}}$, while a narrowing of the potential increases the coupling to rotations. For translations, all changes to the potential resulted in an increased energy transfer, reflecting an increased collision velocity.

The last issue we consider in the dependence of the energy exchange as a function of temperature, is the effect of the cluster potential (we showed the b dependence above). Previously, the energy exchange in the limit of large collision energies[17] has been shown to be influenced by the intra-cluster potential. Here we investigate this problem by comparing the results of helium collisions with Pd_{13} with helium collisions with the soft potential. The energy exchange is shown in Fig. 7 for two different temperatures, 100 and 500 K. We notice that the two potentials have very different melting temperatures, the Pd_{13} cluster shows a rigid-fluid transition at about 1000 K,[13] while the soft potential cluster (sodium parameters with palladium mass) has this transition at about 320 K.[25] This gives that the cluster with this soft potential is in a liquid state at 500 K, while both clusters are rigid at 100 K.

The effect of a softer cluster potential is a clear enhancement of the collision efficiency. For the hard potential case, the effect of having the cluster at different temperatures is more or less a rigid shift of the energy transfer curve. For the soft potential, however, we demonstrate that a more efficient energy transfer is obtained having the cluster in a liquid state. The overall larger energy transfer for the soft potential is in qualitative agreement with the simple model by Mahan,[10] emphasizing the crucial importance of characteristic vibration frequencies for the energy transfer.

B. Cluster cooling

In addition to the studies of how potentials, masses, and temperature influence the energy transfer efficiency, we studied the cooling of clusters using noble gas collisions. This is an essential issue in the understanding of the performance of cluster sources. It is also interesting from a computational point of view, since most simulations at constant temperature are done with thermostats such as the Nosé–Hoover thermostat.[26] In a previous publication,[13] we compared a noble-gas collisional thermostat with the Nosé–Hoover method, and found that the Nosé–Hoover approach surely mimics the more physical collisional heating.

An observation from the results presented above (Fig. 7), is that the energy exchange actually is linear with the gas temperature for the simulation of helium collisions with the model cluster. Furthermore, the slopes of the curves are al-

most independent of the cluster temperature, as long as they are rigid. Thus, the *mean* energy transfer seems to be captured by an expression: $\overline{\epsilon} = k \cdot (T_g - T_c)$, where k is the average slope in Fig. 7. k, which we call the energy exchange constant, is a function of atomic mass, cluster mass, and interaction strengths. When estimating the effect on the cluster temperature on a collision, one should recognize that approximately half of the energy transferred to the cluster results in changes of the internal potential energy,[27] and only half of the transferred energy gives a change of the cluster temperature. The temperature change (ΔT) in one collision can therefore be estimated by

$$\frac{3n}{2} k_b \Delta T = \frac{k}{2} \cdot (T_g - T_c), \tag{11}$$

where n is the number of atoms in the cluster. We notice that this expression in the limit of $k/3k_b = 1$ reduces to the energy transfer predicted by the strong collision assumption,[11] known from theories of unimolecular reactions. Using the expression in (11) we arrive at a difference equation for the cluster temperature. The cluster temperature after m collisions is given by

$$T_c(m) = (T_c(0) - T_g) \cdot \left(1 - \frac{k}{3nk_b}\right)^m + T_g . \tag{12}$$

This is a simple expression, which suggests that, for example, about 2500 collisions are needed to cool a Pd_{13} cluster from 600 to 100 K. Experimentally, it is often the pressure that is the known quantity. In Appendix C we show how Eq. (12) can be converted into an expression depending on noble gas pressure and temperature.

To verify the simple difference equation, we performed another set of simulations where temperature of a Pd_{13} cluster was investigated as a function of gas collisions. To simulate this cooling process, the cluster was translated to the origin after every collision event, keeping the atomic velocities unchanged so as to allow both vibrations and translations/rotations of the cluster. b and v were generated according to physical distributions $f_b(b)$ and $f_v(v)$ corresponding to $T_g = 100$ K. Figure 8 shows the result of single helium atoms colliding with a Pd_{13} cluster. In the lower panel the cluster is initially at a temperature of 600 K. In this case, all degrees of freedom have the same temperature, i.e., a rigid rotation and translation are initially added to the cluster. For the total cluster temperature, the results from the simulation follow the simple expression in Eq. (12), using the energy exchange constant k derived from the simulations above. A relevant question is whether the same k could be used in simulations of different cluster sizes. We checked this by cooling an icosahedral Pd_{55} cluster from 800 K with a 100 K buffer gas, and found that the cluster temperature was fairly well described by Eq. (12) with k derived from the Pd_{13} simulations.

In the upper panel of Fig. 8, the cluster temperature is initially at 1500 K, with zero temperature in rotations and vibrations. This is a temperature that is about 500 K above the melting transition in Pd_{13}. The temperature evolves also

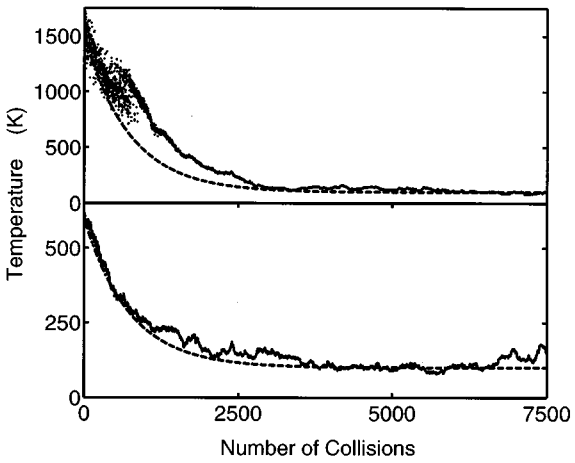

FIG. 8. Cooling of Pd_{13} with collisions by helium.

in this case close to the solutions of Eq. (12), giving a somewhat slower convergence due to the ''liquid'' to ''rigid'' transition. The ''freezing'' transition is clearly seen in our data, signaling a temperature region in which the cluster temperature follows two different cooling curves. The region of about 250 K, agrees well with the co-existence region, previously attributed to Pd_{13}.[13] The cooling rate in the simulation is about 20 K/ns, which is slow enough to get a physical description of the thermal transition. The co-existence region[28] is an effect of barriers separating different regions of the phase space. The clusters can be trapped in some region at a given temperature, and cannot come into contact with other regions corresponding to a different thermal phase of the cluster. The freezing transition is also clearly seen in the total energy versus temperature characteristics not presented here. Clearly, this phenomenon can only be found when the cluster is simulated in a microcanonical ensemble.

IV. CONCLUSIONS

We have used MD simulations to investigate the energy transfer in metal cluster–noble gas atom collisions. By varying the parameters determining the energy exchange we are able to draw some general conclusions: (i) The mass is important for the energy transfer, a larger mass of the noble gas atom results in a larger energy transfer. However, the scaling is not as fast as a hard sphere assumption. (ii) The intracluster potential is very important for the energy transfer. A soft potential gives more efficient transfer than a hard potential does. (iii) In our simulations we obtain a strong dependence on the interaction between cluster and noble gas atoms only in the low temperature limit.

Our results offer a way to estimate the number of collisions needed to control the temperature of clusters by a noble gas atmosphere. Knowing the energy exchange constant, we find that a simple difference equation holds for the estimation of the cluster temperature. We find, for example, that a Pd_{13} cluster is cooled from a liquid state to 100 K, by about 3000 collisions.

ACKNOWLEDGMENTS

We thank Professor Arne Rosén for valuable discussions and continuous support. Several interesting discussions with Professor Sture Nordholm are also acknowledged. The work was supported by NFR (F-Fu 2560-346) and the NUTEK/NFR Material Research Consortia.

APPENDIX A: INITIAL CLUSTER TRANSLATION

The simulations have been performed with zero initial kinetic energy in the rotational and vibrational degrees of freedom. Here we show how it is possible to compensate for the translations, using the present set of data.

If the cluster has an initial translation, w, the distribution of the collisional speed is changed from $f_v(v,T_g)$ into $f_{vw}(v_r,w,T_g)$, where v_r is the relative speed between the gas atoms and the cluster. The new distribution function with the cluster speed w is

$$f_{vw}(v_r,w,T_g) \propto \int_0^{2\pi} d\phi \int_0^{\pi} d\theta^3 \; v_r e^{-m(\mathbf{v}+\mathbf{w})^2/2k_bT_g} \sin\theta, \tag{A1}$$

m being the gas atom mass.

When this new function $f_{vw}(v_r,w,T_g)$ has been evaluated, we can recalculate $g_i(T_g)$ in Eq. (7) according to

$$g_i(T_g) = \frac{f_b(b_i) f_{vw}(v_r,w,T_g)}{\tilde{f}_b(b_i)\tilde{f}_v(v_i)}, \tag{A2}$$

and, thus, obtain $\overline{\epsilon}$ using the original set of data $\{v_i,b_i,\epsilon_i\}$.

However, in the source the clusters are in the form of a gas with different speeds w, corresponding to the temperature $T_{c,cm}$. If the concentration of the cluster is low relative to the concentration of the noble gas, each cluster can be considered as being a beam and the results above are valid for each cluster,

$$f_{vw}(v_r,T_g,T_{c,cm}) \propto \int_0^{\infty} dw \; w^2 e^{-Mw^2/2k_bT_{c,cm}} \int_0^{2\pi} d\phi \cdot \int_0^{\pi} d\theta \; v_r^3 e^{-m(\mathbf{v}+\mathbf{w})^2/2k_bT_g} \sin\theta, \tag{A3}$$

M is the mass of the cluster, and $T_{c,cm}$ is the center of mass temperature of the cluster.

The graphs for $f_{vw}(v_r,T_g,T_{c,cm})$ with T_g equal to 500 K, and $T_{c,cm}$ equal 0, 500, and 1500 K, respectively, are shown in Fig. 9 for the case of Pd_{13}. There is no difference between f_v and f_{vw} in the 0 and 500 K cases, while a slight influence of the center of mass temperature is observed with 1500 K. Thus, we may conclude that an initial zero cluster speed has a minor effect on our results.

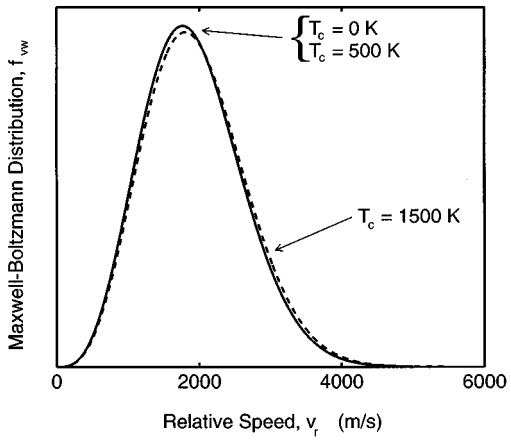

FIG. 9. The dependence of f_{vw} on the different cluster center of mass temperatures.

APPENDIX B: DOUBLE COLLISIONS

Only single atom collisions occur in our simulations. It is therefore important to investigate the probability for double or higher atom collisions as a function of gas pressure and temperature, p_g and T_g.

The gas atoms have a collision time, $\tau(v)$, which we regard as the time from the start at the cut-off limit until the sampling period is over. The collision time increases when v decreases. It is reasonable to assume that simultaneous collisions do not affect $\tau(v)$. The probability for single collisions, $P(s)$, is then

$$P(s) = e^{-z\int_0^{\infty} dv f_v(v,T_g)\tau(v)} \cdot \int_0^{\infty} dv \; f_v(v,T_g) e^{-z\tau(v)}; \tag{B1}$$

z is the number of collisions per second (Appendix C).

The probability is dependent on $b_{\max}$ since z increases if $b_{\max}$ becomes larger. From our simulations we obtained $\tau(v)$. We find that the maximum τ for a given v may be modeled with an exponential function. Using this fit will underestimate the pressure limit for multi atom collision. With the fitted $\tau(v)$ we find that at $T_g = 500$ K, more than 98% of the collisions are single collisions if P_g is less than 150 mbar. The pressure in a cluster source is usually about 100 mbar.

APPENDIX C: PRESSURE DEPENDENCE

The energy transfer from the noble gas to the cluster may also be expressed as a function of time and pressure. Considering the center of mass speed of the clusters to be zero, the number of collisions per second between a specific cluster and noble gas atoms, z, is

$$z = p_g \sqrt{\frac{8\pi}{mk_bT_g}} b_{\max}^2. \tag{C1}$$

The total energy transfer per second to a cluster, $\overline{\epsilon_p}$, is obtained as

$$\overline{\epsilon_p} = z \cdot \overline{\epsilon} = p_g \sqrt{\frac{8\pi}{m k_b T_g}} b_{\max}^2 \overline{\epsilon} = p_g \sqrt{\frac{8\pi}{m k_b T_g}} b_0^2 \overline{\epsilon}_{\text{norm}}, \tag{C2}$$

which is independent on $b_{\max}$.

[1] K. E. Schriver, J. L. Persson, E. C. Honea, and R. L. Whetten, Phys. Rev. Lett. **64**, 2539 (1990).
[2] W. A. de Heer, P. Milani, and A. Chatelain, Phys. Rev. Lett. **65**, 488 (1990).
[3] L. Holmgren and A. Rosén (unpublished).
[4] T. G. Dietz, M. A. Duncan, D. E. Powers, and R. E. Smalley, J. Chem. Phys. **86**, 3911 (1981).
[5] H. Haberland, *Clusters of Atoms and Molecules*, edited by H. Haberland (Springer-Verlag, Berlin, 1994).
[6] P. Milani and W. A. de Heer, Phys. Rev. B **44**, 8346 (1991).
[7] M. Y. Hahn and R. L. Whetten, Phys. Rev. Lett. **61**, 1190 (1988).
[8] D. Tománek, S. Mukherjee, and K. H. Bennemann, Phys. Rev. B **28**, 665 (1983); **29**, 1076 (E) (1984).
[9] W. Zhong, Y. S. Li, and D. Tománek, Phys. Rev. B **44**, 13 053 (1991).
[10] B. H. Mahan, J. Chem. Phys. **10**, 5221 (1970).
[11] C. N. Hinselwood, Proc. R. Soc. London Ser. A, **113**, 230 (1927).
[12] E. K. Grimmelmann, J. C. Tully, and M. J. Cardillo, J. Chem. Phys. **72**, 1039 (1980).
[13] H. Grönbeck, D. Tománek, S. G. Kim, and A. Rosén, Chem. Phys. Lett. **264**, 39 (1997).
[14] See, e.g., I. Oref and D. C. Tardy, Chem. Rev. **90**, 1407 (1990).
[15] L. Ming, J. Davidsson, and S. Nordholm, Chem. Phys. **201**, 121 (1995).
[16] J. Schulte, R. R. Lucchese, and W. H. Marlow, J. Chem. Phys. **99**, 1178 (1993).
[17] P. de Sainte Claire and W. L. Hase, J. Phys. Chem. **100**, 8190 (1996); P. de Sainte Claire, G. H. Peslherbe, and W. L. Hase, *ibid.* **99**, 8147 (1995).
[18] J. Schulte and G. Seifert, Chem. Phys. Lett. **221**, 230 (1994).
[19] W. Zhong, Y. Cai, and D. Tománek, Phys. Rev. B **46**, 8099 (1992); W. Zhong, Y. Cai, and D. Tománek, Nature **362**, 435 (1993).
[20] G. L. Estiú and M. C. Zerner, J. Phys. Chem. **98**, 4793 (1994).
[21] The potential parameters for sodium are $\xi_0 = 0.5176$ eV, $\epsilon_0 = 0.05350$ eV, $p = 9$, $q = 3$, and $r_0 = 3.66$ Å.
[22] *Numerical Recipes*, edited by W. H. Press, S. A. Teukolsky, W. T. Vetterling, and B. P. Flannery (Cambridge University Press, Cambridge, 1992).
[23] D. G. Leopold, J. Ho, and W. C. Lineberger, J. Chem. Phys. **86**, 1715 (1987).
[24] The energy expression for energy exchange in hard sphere collisions is $\Delta E = 1 + \{4(1-(b/D)^2)/[m/M+1]\}[1/(m/M+1)-1]$. Here, b is the impact parameter, D is the sum of the hard sphere radii for the cluster and the atom. m and M are the masses for the atom and the cluster, respectively.
[25] J. Westergren, H. Grönbeck, S. G. Kim, and D. Tománek (unpublished).
[26] S. Nosé, J. Chem. Phys. **81**, 511 (1984); W. G. Hoover, Phys. Rev. A **31**, 1695 (1985).
[27] We checked this assumption in the case of helium collisions with Pd_{13}. An average of k_{pot} in Fig. 7 is 2.0 μeV/K, which could be compared with the value of k_{tot} which is 4.3 μeV/K.
[28] R. S. Berry, J. Jellinek, and G. Natanson, Phys. Rev. B **30**, 919 (1984); T. L. Beck, J. Jellinek, and R. S. Berry, J. Chem. Phys. **87**, 545 (1987).